

## Sedimentation Field Flow Fractionation of Mitochondrial and Microsomal Membranes from Corn Roots

SAMUEL M. MOZERSKY,<sup>1</sup> KARIN D. CALDWELL,\* SUSAN B. JONES,  
BEVERLY E. MALEEFF, AND ROBERT A. BARFORD

*Eastern Regional Research Center, U. S. Department of Agriculture, ARS, 600 East Mermaid Lane, Philadelphia, Pennsylvania 19118, and \*Department of Bio-engineering, University of Utah, Salt Lake City, Utah 84112*

Received November 27, 1987

Sedimentation field flow fractionation (sed-FFF) is shown to be a valuable procedure for analysis of a wide variety of subcellular particle preparations. The principles underlying this relatively new separation procedure are described. Separation is based on differences between particles in mass and/or density. As in chromatography, the procedure involves relating on-line or off-line measurements made on the effluent from the separation chamber to the elution (retention) time. In this work effluents were monitored for absorbance at 254, 280, and/or 320 nm; collected fractions were assayed for protein content, total ATPase activity, and/or marker enzyme activities and, when appropriate, were examined by electron microscopy. The ratio of the absorbances at 254 and 320 nm was found to provide a sensitive measure of partial resolution of subcellular particles. Preparations containing all of the subcellular particles of corn roots (exclusive of nuclei, cell walls, and ribosomes), and fractions thereof enriched in mitochondria, microsomes, Golgi membranes, or plasma membranes, were examined by sed-FFF. The subcellular particles appear to remain largely intact. All of the particles observed had a mass less than  $2 \times 10^{11}$  g/mol. All of the preparations were grossly heterogeneous with respect to effective mass distribution. This is due in part to heterogeneity with respect to the organelle of origin. In microsome preparations, components of low, medium, and high density were present in the unretained peak; the retained region had comparatively more high density particles. Plasma membrane preparations had a very wide effective particle mass distribution. The observations suggest that, in addition to its utility for analytic purposes, sed-FFF is likely to prove useful for micro-preparative fractionation of some subcellular particle preparations. Sed-FFF and density gradient centrifugation can be utilized as complementary methods. © 1988 Academic Press, Inc.

**KEY WORDS:** subcellular fractionation; microsomes; cell organelles; membrane isolation; membrane structure; field flow fractionation.

Sedimentation field flow fractionation has been shown to be an effective separation procedure for particles of a very broad mass range, ca.  $10^6$  to  $10^{12}$  g/mol (1,2), and has been applied to the fractionation of cells (3), bacterial cell wall fragments (4), and DNA (5). The gentleness of the procedure, the absence of a support medium, and the mass range covered suggested to some of us (6)

that sed-FFF<sup>2</sup> may be useful for the fractionation of subcellular particles, i.e., organelles

<sup>2</sup> Abbreviations used:  $A_\lambda$ , absorbance at wavelength  $\lambda$  (in nm); DG, density gradient; DTT, dithiothreitol (1,4-dimercapto-2,3-butanediol); ER, endoplasmic reticulum; FFF, field flow fractionation; G, Golgi; Hepes, 4-(2-hydroxyethyl)-1-piperazineethanesulfonic acid; ME, 2-mercaptoethanol; Mes, 2-(*N*-morpholino)ethanesulfonic acid; Ms, microsome(s); Mt, mitochondria; PACP, periodic acid-chromic acid-phosphotungstic acid; PM, plasma membrane; sed-FFF, sedimentation-FFF;  $\rho$ , density.

<sup>1</sup> To whom all correspondence should be addressed.

and particles derived from them. Such particles are frequently fragile, and many of them fall in the weight range  $10^8$  to  $10^{12}$  g/mol and the size range 0.1 to 1.0  $\mu\text{m}$ . Rapid fractionation procedures to evaluate such preparations are sorely needed. In this communication we show that sed-FFF is, indeed, a convenient and efficient procedure for the analysis of a wide variety of subcellular particle preparations. Our results suggest that the procedure is also likely to be useful for micro-preparative fractionation of such preparations.

### Theory of Sedimentation Field Flow Fractionation

Since the fundamental concepts involved in sed-FFF are not generally known, they are reviewed here.

Separation takes place in a ribbon-like cavity or channel in the rotor of a centrifuge (2,7) through which carrier (solvent) is flowing at a uniform velocity (Fig. 1). After the channel is filled with carrier, the sample is introduced into the channel as a uniform suspension or solution of particles suspended or dissolved in the carrier. Once the sample has entered the separation channel, carrier flow is stopped, while the centrifugal field  $G$  is held at its initial value  $G_0$ , until sedimenta-

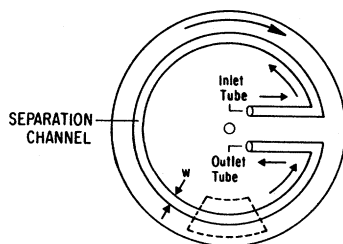


FIG. 1. A cross-sectional view of the rotor of a sedimentation field flow fractionator. The channel dimensions are 90 ( $l$ )  $\times$  2.25 ( $h$ )  $\times$  0.0254 cm ( $w$ ). The width  $w$  is shown on the diagram. The "height"  $h$  of the channel is the dimension perpendicular to the plane of the drawing. The length  $l$  is the distance along the circular path from channel inlet to outlet. The portion of the channel enclosed in the small rectangle (dotted lines) is enlarged in Fig. 2.

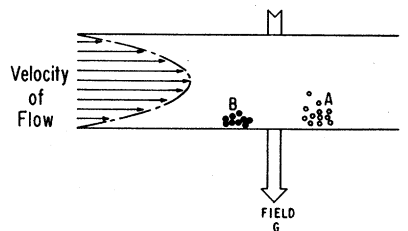


FIG. 2. An enlarged view of a section of the separation channel (Fig. 1) showing the direction of the field, the flow profile, and the separation of two species of particles, A and B.

tion equilibrium is achieved, i.e., until the particle concentration at every point in the channel is invariant with time (disregarding longitudinal diffusion). Carrier flow is then resumed. The period during which carrier flow is interrupted to allow for equilibration is called the relaxation period.

Figure 2 shows an enlargement of the portion of the channel highlighted in Fig. 1, after substantial separation has taken place. Carrier flow is slow and therefore laminar, with a parabolic profile (1), as shown. The externally imposed centrifugal field  $G$  has moved the suspended or dissolved particles radially (downward in Fig. 2), so that they accumulate at one wall of the channel, the accumulation wall; this is usually the outer wall. Each particle is assumed to move through the channel longitudinally, i.e., counter-clockwise in Fig. 1 and left to right in Fig. 2, with the local velocity of the carrier.

As a result of the balance, at equilibrium, between the opposing actions of the field and diffusion, the concentration ( $c$ ) of each species of particle is maximal ( $c_0$ ) at the accumulation wall ( $x = 0$ , Figs. 2 and 3) and falls exponentially as we move away from the wall and into the channel (8). The concentration distributions are shown (Fig. 3) for two species, A and B, the first consisting of relatively small, light particles and the second of relatively large, dense particles. Species unaffected by the field, e.g., those having the same density as the carrier, remain uniformly distributed across the channel.

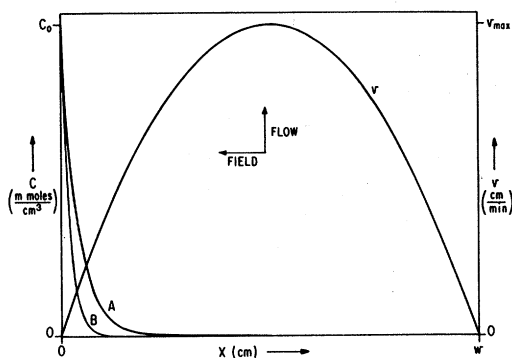


FIG. 3. The concentration distributions ( $c$ ) for species A and B of Fig. 2, and the velocity (flow) profile ( $v$ ) in the separation channel.

The longitudinal velocity profile seen in Fig. 2 is shown again in Fig. 3. For a given species of particle, the flux density  $J$  in the longitudinal direction at any level  $x$  is given by  $J(x) = v(x) c(x)$ . If  $v$  is the local linear velocity in the channel in centimeters per minute and  $c$  is the concentration in millimoles per cubic centimeter (molarity), the flux  $J$  is in millimoles per minute per square centimeter cross-sectional area.  $J(x)$  is plotted for species A and B in Fig. 4a. The average linear velocity  $\langle v \rangle$  of each species is given by the ratio of the average flux  $\langle J \rangle$  to the average concentration  $\langle c \rangle$ :  $\langle v \rangle = \langle J \rangle / \langle c \rangle$ ,  $\langle J \rangle$  and  $\langle c \rangle$  being obtained from the distri-

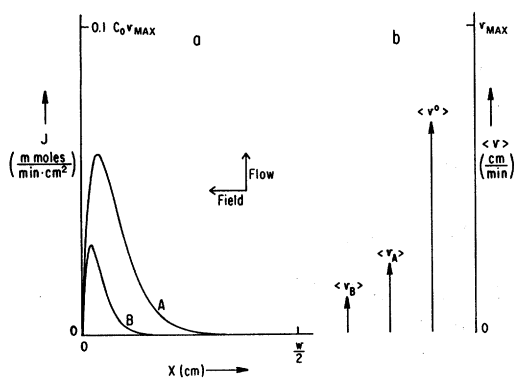


FIG. 4. (a) The instantaneous flux density ( $J$ ) for species A and B of Figs. 2 and 3 as a function of position ( $x$ ) in the channel. (b) The average velocities of species A and B and of the carrier (solvent). (Note that there is no abscissa for Fig. 4b.)

butions of  $J$  and  $c$  shown in Figs. 4a and 3, respectively.

The values of  $\langle v \rangle$  for species A and B are plotted in Fig. 4b. For the carrier,  $\langle v \rangle = \langle v^0 \rangle = 2v_{\max}/3$ . For particles unaffected by the field,  $\langle v \rangle = \langle v^0 \rangle$ .

Since the channel width  $w$  is very small, diffusion in the lateral ( $x$ ) direction is very significant. Although the exponential concentration distribution of Fig. 3 holds, rapid lateral ( $x$ -direction) interchange among particles of a given species can be assumed, so that over any substantial time interval all particles of a given species move longitudinally with essentially the same velocity, the average velocity  $\langle v \rangle$ .

How far the particles of a given species are, on the average, from the wall at which they accumulate depends not only on the species of particle, i.e., its size and density, but also on the field strength  $G$ , being inversely proportional to the latter (8). However, a field which is large enough to appreciably affect particles of moderate size and density forces large, dense particles to pack tightly close to the accumulation wall. This gives rise to a very small  $\langle v \rangle$  and an excessively long elution time  $t_e$  (very high retention), which yields a broad, flat peak. To overcome these disadvantages, the field  $G$  is allowed to decay exponentially (9), after an initial period of duration  $t_c$  during which it is held constant at  $G_0$  (Fig. 5). As  $G$  decreases, the particles

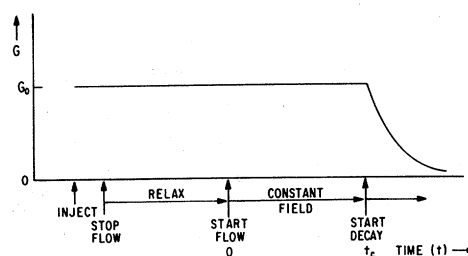


FIG. 5. A two-phase field program: constant field  $G_0$  for time  $t_c$  followed by exponential decay with decay constant  $\tau$ . For corn root membranes, typical values chosen were  $G_0$ ,  $4.4 \times 10^4$ – $3.9 \times 10^5$  cm/s<sup>2</sup> (500–1500 rpm); relaxation time, 5–20 min;  $t_c$ , 10–15 min;  $\tau$ , 5–15 min.

move away from the wall,  $\langle v \rangle$  (Fig. 4) therefore increases, and the elution time  $t_e$  (retention time) is reduced. The adjustments in particle position  $x$  and in  $\langle v \rangle$  to changing  $G$  are usually assumed to be instantaneous.

Assuming reasonably high retention, equations relating the effective (buoyancy-corrected) molar mass  $M_{\text{eff}}$  to the elution (retention) time  $t_e$  can be derived (cf. Ref. (9), Eqs. 5 and 14). For components eluting before field decay, while  $G = G_0$  and  $2t_0 < t_e \leq t_c$ ,

$$M_{\text{eff}} = M(\rho_p - \rho_0)/\rho_p = (6R_0T/wG_0t_0)t_e. \quad [1]$$

For those eluting during the decay phase,  $t_e \geq t_c$ ,

$$M_{\text{eff}} = M(\rho_p - \rho_0)/\rho_p = (6R_0T/wG_0t_0) \times \{t_c + \tau[\exp((t_e - t_c)/\tau) - 1]\}. \quad [2]$$

In these equations  $M$  is the mass of 1 mol of particles (g/mol, daltons) (for substances dispersed as molecules,  $M$  is the molecular weight);  $\rho_p$  is particle density (g/cm<sup>3</sup>);  $\rho_0$ , carrier density;  $R_0$ , the gas constant (erg/deg mol);  $T$ , the absolute temperature (deg);  $w$ , the channel width (cm);  $G_0$ , the initial centrifugal field strength (cm/sec<sup>2</sup>);  $t_0$ , the elution (retention) time for unretained particles;  $t_c$ , the period of time after relaxation during which the field is held constant at  $G_0$ ;  $\tau$ , the field decay constant; and  $t_e$ , the elution (retention) time for particles of mass  $M$  and density  $\rho_p$ .

As in chromatography, the raw data obtained from FFF relate a detector signal, which is a measure of concentration, either to elution (retention) time  $t_e$  or to a fraction number, which corresponds to an average elution time. Every elution time is, by Eqs. [1] and [2], characteristic of a particular effective mass  $M_{\text{eff}} = M(\rho_p - \rho_0)/\rho_p$ . If a particle density  $\rho_p$  is assumed (10),  $M$  can then be calculated from the effective mass. Alternatively,  $M$  and  $\rho_p$  can, in principle, be obtained by making two sed-FFF runs at different carrier densities, so that a pair of simulta-

neous equations for  $M(\rho_p - \rho_0)/\rho_p$  is obtained.

For low retention, Eq. [1] is not valid (nor is Eq. [2]). In this case, for  $t_e < t_c$  the effective molar mass (molecular weight)  $M_{\text{eff}}$  can be related to the retention ratio  $R$  by the following more general equations (Eqs. 7 and 9 of Ref. (8)),

$$\lambda = \frac{R_0T\rho_p}{MG_0w(\rho_p - \rho_0)} = \frac{R_0T}{M_{\text{eff}}G_0w} \quad [3]$$

and

$$R = 6\lambda[\coth(1/2\lambda) - 2\lambda] \quad [4]$$

where  $R = t_0/t_e$ . For Eq. [3], the ratio of Boltzmann's constant to particle mass,  $k/m$  in Ref. (8), was replaced by the ratio of the gas constant to the molar mass,  $R_0/M$ . Equations [3] and [4] were always used to obtain  $M_{\text{eff}}$  for the abscissa scale in the region  $t_e < t_c$ .

## MATERIALS AND METHODS

*Corn root membrane preparations.* All subcellular particle preparations were made from Zea mays L. corn (Illinois Foundation Seeds, Champaign, IL) roots. Twenty-five grams (fresh weight) of corn roots was homogenized (11) in a medium containing 5.0 mM EDTA, 5.0 mM DTT, 5.0 mM ME, 300 mM sucrose, and 100 mM Hepes buffer, pH 7.38  $\pm$  0.15 (25°C). The homogenate was filtered through cheesecloth and centrifuged at 1000g. To make the broad-spectrum preparation containing both Mt and Ms, the 1000g supernatant was centrifuged at 100,000g for 45 min, and the pellet (Mt + Ms) resuspended in 1.8 ml of FFF carrier (see below) per gram pellet. To make a preparation of Mt, the 1000g supernatant was centrifuged at 7000g for 20 min, and the pellet was suspended in 2 ml of FFF carrier. Microsomes were isolated from the supernatant decanted from over the Mt pellet by centrifuging at 100,000g for 35–45 min. To wash the microsomes the Ms pellet was resuspended in the homogenization medium (above) and recentrifuged at 100,000g for

35–45 min. For FFF the Ms pellet, washed or unwashed, as desired, was suspended in 1.5 ml of FFF carrier (see below). When endoplasmic reticulum-, Golgi-, and plasma membrane-enriched preparations were all needed, these were obtained from the microsome fraction by equilibrium centrifugation for 15–17 h on a linear sucrose density gradient (11). When only a PM-enriched preparation was needed, the Ms pellet was resuspended in 1 ml of suspending medium and subjected to step density gradient fractionation (cf. Ref. (12)). The lower layer of the step gradient pair was 14 ml of 45% (w/w) sucrose + 30 mM Hepes buffer, pH 7.5 (5°C) ( $\rho = 1.20 \text{ g/cm}^3$ ), and the upper layer was 22 ml 34% sucrose + 30 mM Hepes buffer ( $\rho = 1.15$ ). After centrifuging at 82,700g for 2 h, the material at the interface between the 34 and 45% sucrose solutions was collected. Golgi-enriched preparations were prepared in the same way as PM-enriched preparations, except that the step gradient was from 30 to 38.5% (w/w) sucrose (density from 1.13 to 1.17  $\text{g/cm}^3$  (see Ref. (10)).

All preparative operations subsequent to excision of the roots were at 2–5°C.

**Field flow fractionation.** The apparatus used was that described by Giddings *et al.* (7) for sed-FFF and was built at the University of Utah. The separation channel was constructed of Hastelloy C, a corrosion-resistant steel alloy. The dimensions of the channel were  $90 \times 2.25 \times 0.0254 \text{ cm}$ , with a void volume of 5.15 ml; the radius was 15.5 cm. The angular velocity of the rotor was programmed and controlled within 0.5% of the desired level by an LS 11 computer. All runs were made at room temperature (23–26°C). Samples of 400–600  $\mu\text{l}$  were injected directly into the channel through a septum port mounted on the channel block while the rotor was stationary. Carrier solution was pumped by a Gilson Minipulse peristaltic pump at ca. 1 ml/min. For direct monitoring at 254 and 320 nm, two detectors were placed in series; the first was an Altex Model 153 and the second a Schoeffel Spectroflow

SF 770. The output signals were fed to an Omniscrite dual pen recorder from Houston Instrument.

Specific conditions for individual runs are given in the legends to the figures. Usual conditions were relaxation time, 5–20 min; initial rotor velocity, 500–1500 rpm; constant time, 10–15 min; field decay constant, 5–15 min; flow rate, 54 ml/h.

The FFF carrier solution consisted of 1.0 mM DTT, 1.0 mM ME, 300 mM sucrose, and either 3.0 mM Tris–Mes buffer, pH 7.2, or 3.0 mM Hepes buffer, pH  $7.38 \pm 0.15$  (25°C). When the effluent was to be assayed for cytochrome oxidase activity, DTT and ME were omitted, since reducing agents interfere with the assay.

**Assays.** Protein concentration was measured with Coomassie brilliant blue G-250 (Bio-Rad Corp., Richmond, CA, or Sigma Chemical Co., St. Louis, MO) by the Bradford micro-procedure (13).

Marker enzyme activities were measured by the procedures described by Hodges and Leonard (14), except for minor modifications. In the assay for cytochrome oxidase activity, digitonin was replaced by Triton X-100. Latent UDPase, the marker enzyme for Golgi membranes, was measured as the difference in UDPase activity in the presence and absence of 0.03% (w/v) digitonin (Ref. (11) and G. Nagahashi, personal communication).  $\text{K}^+$ -activated ATPase, i.e., the difference in ATPase activities in the presence and absence of  $\text{K}^+$ , was used as a marker for PM (10,14). When the distribution of total ATPase activity in the FFF effluent was desired, only the activity in the presence of  $\text{K}^+$  was measured. Since various ATPases are associated with a wide variety of membranes, including Mt, PM, G, and ER (14), total ATPase activity serves to characterize the FFF effluent with a measure intermediate in specificity between that of an enzyme marker and that of protein concentration. For assay of total ATPase activity, either the procedure of Hodges and Leonard (14) was used or that of Fritz and Hamrick (15); in the latter case,

the  $\text{NAD}^+$  generated was determined by the fluorescence method of Ciotti and Kaplan (Ref. (16), Section IIB).

Corn root membrane preparations contain ADPase and phosphatase activities, as well as ATPase activity; the assay of ATPase via ADP production (15) therefore yields low values for ATPase activity, while measurement of inorganic phosphate (14) gives high values. This is not a serious drawback in the present work, since the inferences drawn from the ATPase data are based only on considerations of relative activity in different parts of the fractogram and how this demonstrates separation.

**Electron microscopy.** Membrane preparations and selected fractions obtained by FFF were diluted with cold, double-strength fixative to give a final concentration of 2.5% glutaraldehyde and 0.05 M sodium cacodylate buffer, pH 7. Samples were fixed for 1.5 h in an ice bath, rinsed with the same buffer, and postfixed with 1% osmium tetroxide in 0.1 M sodium cacodylate buffer, pH 7. After centrifugation at 80,000g, fragments of the pellets were dehydrated in a graded acetone series and embedded in Spurr resin. Thin sections (80 nm) on stainless steel grids were selectively stained for PM enhancement with PACP by the methods of Nagahashi *et al.* (17), except that sections were stained for 20 min at 30°C. Unstained sections served as controls. The specificity of the stain for PM was verified on sections of embedded corn root. The sections were examined with a Zeiss EM-10B transmission electron microscope operating at 60 kV.

## RESULTS AND DISCUSSION

### Mitochondria

Protein ( $c_p$ ) and marker enzyme ( $c_E$ ) fractograms typical of those obtained with preparations of Mt are shown in Fig. 6. The range of effective particle mass,  $M_{\text{eff}}$ , is over 100-fold. At least three populations of particles appear to be present. For the smallest particles  $M_{\text{eff}}$  is less than  $7 \times 10^8$  g/mol; these have

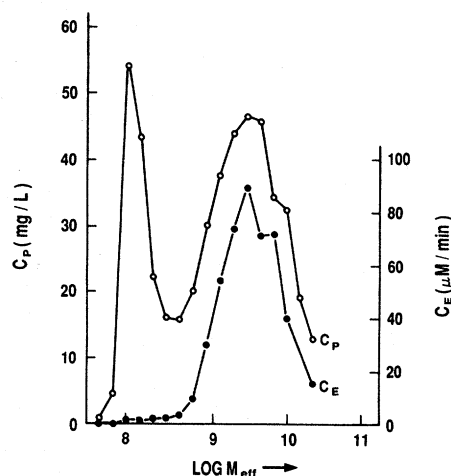


FIG. 6. Protein concentration ( $c_p$ ) and enzyme (cytochrome oxidase) concentration  $c_E$  of the effluent as a function of effective molar mass  $M_{\text{eff}}$  on sed-FFF of a preparation of corn root mitochondria. Conditions of FFF: relaxation time ( $t_{\text{rel}}$ ), 10 min; initial rotor velocity ( $\omega_0$ ), 500 rpm; duration of  $\omega_0$  after relaxation ("constant time"  $t_c$ ), 10 min; field decay constant ( $\tau$ ), 5 min; flow rate ( $f$ ), 54 ml/h.

no cytochrome oxidase activity and are therefore probably not derived from mitochondria. The major retained component peaks at  $2.9 \times 10^9$  g/mol. A second population of retained particles appears as a shoulder on the first; it is centered at ca.  $9.8 \times 10^9$  g/mol. These two populations both have cytochrome oxidase activity, suggesting that there *may* be more than one population of Mt-derived particles in Mt preparations.

If the density of all particles in the preparation is assumed to be that of Mt, viz., 1.19 g/cm<sup>3</sup> (10), the molar mass  $M$  of the smallest particles is less than  $2 \times 10^9$ , the major retained component peaks at  $2.2 \times 10^{10}$ , and the shoulder on the latter is centered at ca.  $7.5 \times 10^{10}$  g/mol.

The protein and enzyme distributions are consistent with the absorbance fractogram obtained (but not shown), including incipient resolution of two retained peaks. There was greater detail in the absorbance fractogram, as one would expect; the latter was obtained on-line with a spectrophotometric

detector having a cell volume of ca. 10  $\mu$ l, while the assays for protein and enzyme content were done on aliquots from fractions having a volume of ca. 1.9 ml.

### Microsome Preparations

Figure 7 shows the fractogram obtained on sed-FFF of a twice-washed preparation of corn root Ms. The gross heterogeneity of this type of preparation is apparent, with at least five components being present. Unwashed Ms preparations were similarly heterogeneous. Washing did not eliminate the void-volume peak, suggesting that low-density and/or small particles ( $M_{\text{eff}} < 1.75 \times 10^8$ ) are present. The elution of particulate material with the void volume was confirmed with a preparation containing Mt as well as Ms (see below).

Assuming the density typical of PM vesicles from nongreen tissue, viz., 1.17 g/cm<sup>3</sup> (18), a particle mass of  $2.6 \times 10^{10}$  Da was obtained for the vesicles at the maximum of the major retained peak ( $M_{\text{eff}} = 3.0 \times 10^9$ ), corresponding to a diameter, for a spherical particle, of ca. 0.45  $\mu$ m. Since the field was turned off just prior to elution of these parti-

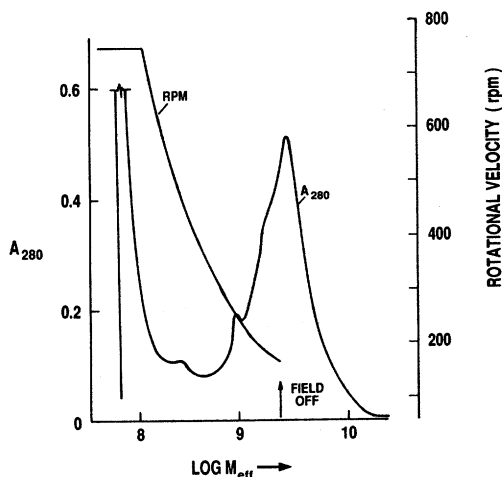


FIG. 7. Fractogram of absorbance at 280 nm ( $A_{280}$ ) on sed-FFF of a preparation of corn root microsomes. Run conditions were  $t_{\text{rlx}}$ , 10 min;  $\omega_0$ , 750 rpm;  $t_c$ , 10 min;  $\tau$ , 10 min;  $f$ , 53 ml/h.

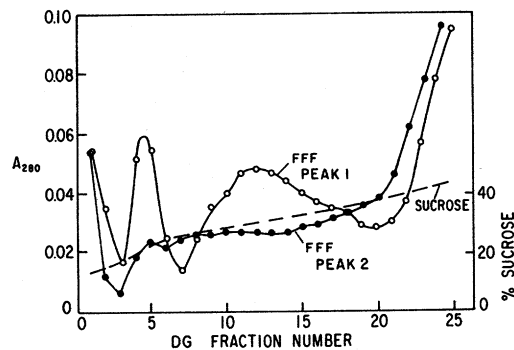


FIG. 8. Analysis by linear density gradient centrifugation of major components not retained (O, peak 1) and retained (●, peak 2) on sed-FFF of microsomes.  $A_{280}$ , absorbance of density gradient fractions at 280 nm.

cles, these estimates may be slightly low. The estimated diameter is within the range 0.2–0.5  $\mu$ m, which includes most microsomal particles (19).

Since  $G$  varies as the square of the rotational velocity, the decay constant  $\tau$  for the field is one-half that for the rotor velocity. Thus, for Fig. 7,  $\tau = 10$  min (see legend), while the decay constant for rotational velocity was 20 min (see curve labeled RPM).

After sed-FFF of a preparation of unwashed microsomes, fractions from peak No. 1, the void-volume peak, and from peak No. 2, the major retained peak of Fig. 7, were separately pooled. Each pooled sample was then subjected to isopycnic sucrose density gradient centrifugation at 80,000g for 15 h (Ref. (11), p. 168). As seen from the  $A_{280}$  DG fractograms in Fig. 8, the compositions of the two major sed-FFF peaks were quite different. Both had substantial amounts of high-density material absorbing at 280 nm. The unretained sed-FFF peak (No. 1) had higher concentrations of low- and medium-density components, and these were clustered into three peaks, with maxima at DG fractions 1, 5, and 12. It is apparent that field-programmed sed-FFF and DG centrifugation are complementary separation procedures; neither accomplishes the separation achieved by the other.

### Plasma Membrane and Golgi Preparations

The fractions obtained on sed-FFF of a PM preparation made by the step gradient method were assayed for protein content and for total ATPase activity (Fig. 9). The maximum protein concentration of the retained peak was less than that of the void-volume peak. Nevertheless the more concentrated of the retained fractions were turbid, while all fractions in the void-volume region were clear. This observation is consistent with the presence of larger, suspended particles in the retained region and a higher content of soluble protein in the void-volume region. In terms of distribution, the protein and enzyme fractograms are generally similar. However, the heterogeneity of the retained components is even more pronounced in the latter. Thus, for example, there appears to be a peak (shoulder) of ATPase activity at  $M_{\text{eff}} = 2.3 \times 10^8$  though there is no corresponding protein peak and the protein concentration is very low.

Since we were dealing primarily with suspended particles which scatter light at wavelengths beyond those at which proteins absorb strongly, the absorbance of the field flow

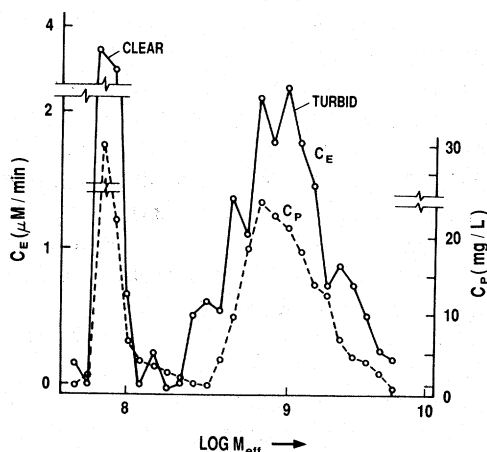


FIG. 9. Protein ( $c_p$ ) and ATPase ( $c_E$ ) concentrations as a function of effective molar mass on sed-FFF of a plasma membrane preparation.  $t_{\text{rx}}$ , 20 min;  $\omega_0$ , 750 rpm;  $t_c$ , 15 min;  $\tau$ , 10 min;  $f$ , 52 ml/h. The field was not turned off until after the last fraction had eluted.

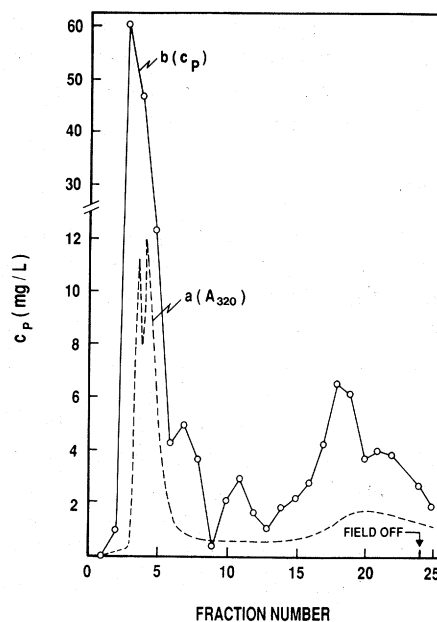


FIG. 10. Particulate and protein distribution on sed-FFF of a Golgi preparation. (a) Fractogram of absorbance at 320 nm, demonstrating partial separation of slightly retained particulates from unretained components; (b) protein concentration distribution. Cleavage in the void-volume region as seen in (a) was demonstrated repeatedly with other preparations. Conditions:  $t_{\text{rx}}$ , 20 min;  $\omega_0$ , 750 rpm;  $t_c$ , 15 min;  $\tau$ , 10 min;  $f$ , 52.8 ml/h.

effluent was monitored at 320 nm, as well as at 254 nm. Figure 10a shows the  $A_{320}$  fractogram for a Golgi-enriched preparation. Whereas in the void-volume region (fractions 1–6) of the 254-nm on-line fractogram (not shown) there was only a suggestion of heterogeneity, the 320-nm fractogram showed clear cleavage. Resolution of slightly retained from unretained components could very likely be improved by increasing the initial field strength.

The positions of these two peaks relative to the starting point give a retention ratio  $R$  for the slightly retained peak of 0.81. Since this peak emerged while the field was held constant, the average particle size of the slightly retained components can be estimated from  $R$  utilizing Eqs. [3] and [4]. Assuming  $\rho_p = 1.15 \text{ g/cm}^3$  (see Golgi in Ref. (10)), and

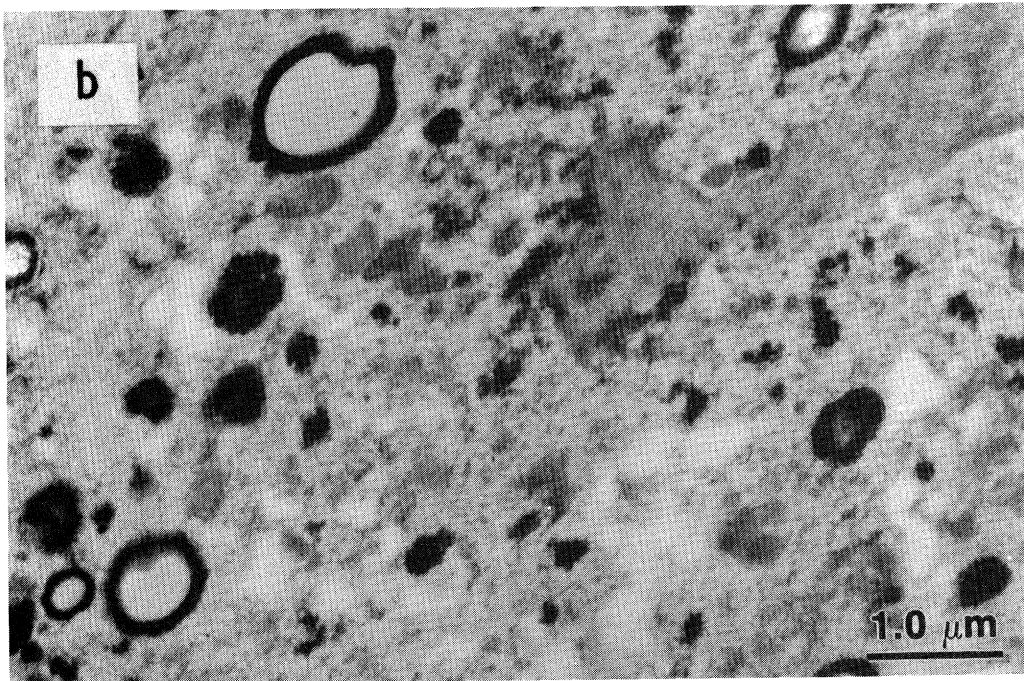
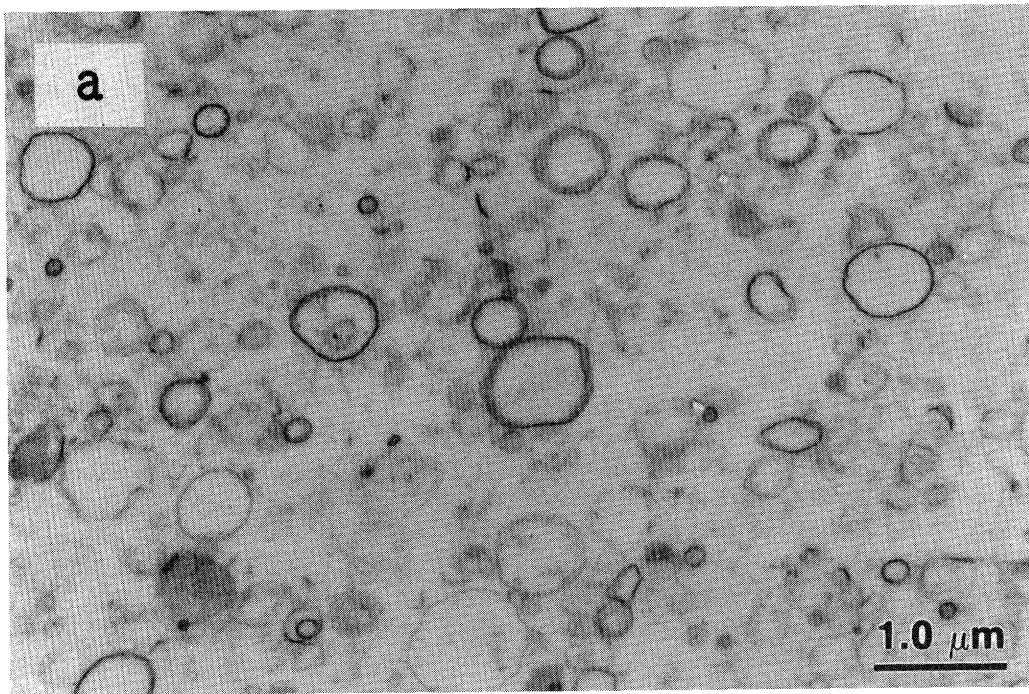


FIG. 11. Electron micrographs of adjacent fractions in the region of the void volume from a preparation of Mt + Ms. Thin sections were stained for PM with PACP. (a) Fraction 3, obtained on the upslope of the "void-volume" peak, showing typical PM vesicles. (b) Fraction 4, containing slightly retained components and devoid of the typical PM vesicles. Conditions for sed-FFF:  $t_{th}$ , 10 min;  $\omega'_0$ , 1500 rpm;  $t_c$ , 10 min;  $\tau$ , 10 min;  $f$ , 54 ml/h.

knowing  $\rho_0 = 1.034$ , a particle mass  $M$  of  $3.8 \times 10^8$  Da was obtained. This compares to  $M < 2.3 \times 10^8$  for particles eluting in the void volume, i.e., those not appreciably affected by the field  $G$ . It may be noted that, had  $M$  for the slightly retained peak been calculated from Eq. [1], the equation commonly used for constant field conditions, it would have been overestimated by 88%.

Assay of the effluent fractions for protein content gave the distribution seen in Fig. 10b. As in the 254-nm fractogram (not shown), there is only a suggestion of heterogeneity in the first peak (fractions 1–6). This is very likely due to the loss of resolution incurred by the collection process, the fraction volume being much greater than the volume of the flow cell in the monitor as previously indicated. Resolution for components eluting early and assayed off-line was improved in later runs by reducing the fraction volume for those fractions eluting early.

#### *Heterogeneity in the "Void-Volume" Region*

The presence of slightly retained components in the later portion of the first peak (Fig. 10a) prompted us to examine, by electron microscopy, the fractions collected on the upslope (fraction 3) and downslope (fraction 4) of this peak, as well as more strongly retained fractions of the effluent. For this purpose we used a preparation of Mt + Ms. Electron micrographs of PACP-stained sections (Fig. 11), showed that the compositions of fractions 3 and 4 are markedly different. The latter contains none of the typical thin-walled PM vesicles present in the former. Fraction 4 contains stained vesicles, but the walls of these vesicles are much thicker than those in fraction 3, and there is a considerable amount of nonvesiculated material that took up the PACP stain. More highly retained fractions (not shown) contained typical PM particles, but in relatively smaller numbers than in fraction 3.

The information on effluent composition provided by the  $A_{320}$  fractogram can be effec-

tively extended by calculating and plotting  $A_{254}/A_{320}$ . The fractogram obtained in this way for a PM preparation is shown in Fig. 12. Homogeneity in any region of the fractogram is indicated by constancy of the absorbance ratio. A substantial change in this value is strong evidence of the separation of different components. Thus, the region of fractions 3–7 is grossly heterogeneous, with at least five components being indicated. By contrast, the absorbance ratio in fractions 11–21 gives no clear indication of heterogeneity. However, here the protein fractogram (not shown) shows that there are at least four components in this region.

The separation of two populations by sed-FFF is based on a difference between them in particle mass or density, or both. Subcellular particles derived from a given species of organelle may exhibit a wide distribution of particle size, even if the particle density is quite uniform. Heterogeneity observed by absorbance and protein fractograms therefore derives from two sources, (i) a difference in particle size, and (ii) a difference in the species of organelle from which the particles are derived. Distinguishing between these requires specific methods, such as assay for marker enzymes and electron microscopy.

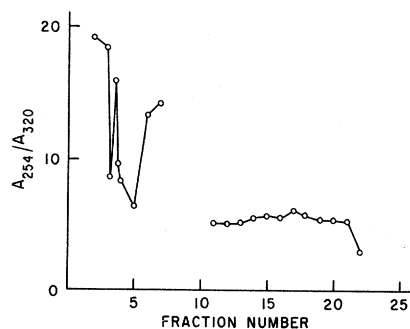


FIG. 12. Fractogram of the ratio of absorbances at 254 and 320 nm for sed-FFF of a PM preparation. The absorbance ratio was not calculated for fractions 1, 8–10, and 23–26 because the absorbance values were very low, rendering the ratio virtually meaningless. Conditions for FFF:  $t_{\text{th}}$ , 20 min;  $\omega'_0$ , 750 rpm;  $t_c$ , 15 min;  $\tau$ , 5 min;  $f$ , 54 ml/h. The field was turned off at fraction 18.

As a check on the extent to which subcellular particles eluted from the field flow fractionator remain intact, we measured the protein content and the ATPase content of fractions or pooled fractions of the PM effluent before and after sedimentation at 80,000g for 2 h. The bulk of the protein and enzyme was particle-bound. This was true even in the earliest eluting material, where particles, such as soluble proteins, less than  $10^8$  Da in mass elute.

Since longitudinal flow through the separation channel, i.e., elution, is inherent to the separation process in FFF, the procedure is fundamentally (micro-) preparative as well as analytical. However, in practice the preparative value of the procedure is sometimes limited because retained components in the effluent are frequently more dilute than those in the injected sample by about two orders of magnitude. The desired particles in the effluent must then be concentrated, while the concentration of the carrier components is kept at tolerably low levels. A stream splitter designed to avoid such extensive dilution exists (20,21), but is not generally available.

#### REFERENCES

- Giddings, J. C., Fisher, S. R., and Myers, M. N. (1978) *Amer. Lab.* **10**, 15-31.
- Kirkland, J. J., and Yau, W. W. (1982) *Science* **218**, 121-127.
- Caldwell, K. D., Cheng, Z. Q., Hradecky, P., and Giddings, J. C. (1984) *Cell Biophys.* **6**, 233-251.
- Fox, A., Schallinger, L. E., and Kirkland, J. J. (1985) *J. Microbiol. Methods* **3**, 273-281.
- Schallinger, L. E., Yau, W. W., and Kirkland, J. J. (1984) *Science* **225**, 434-437.
- Caldwell, K. D., Mozersky, S. M., Nagahashi, G., and Barford, R. A. (1986) in *Chemical Separations* (King, C. J., and Navratil, J. D., Eds.), Vol. 1, pp. 59-74, Litarvan Literature, Arvada, CO.
- Giddings, J. C., Myers, M. N., Caldwell, K. D., and Fisher, S. R. (1980) in *Methods of Biochemical Analysis* (Glick, D., Ed.), Vol. 26, pp. 79-135, Wiley, New York.
- Giddings, J. C., Yang, F. J. F., and Myers, M. N. (1974) *Anal. Chem.* **46**, 1917-1924.
- Yau, W. W., and Kirkland, J. J. (1981) *Sep. Sci. Technol.* **16**, 577-605.
- Quail, P. H. (1979) *Annu. Rev. Plant Physiol.* **30**, 425-484.
- Nagahashi, J., and Kane, A. P. (1982) *Protoplasma* **112**, 167-173.
- Tu, S.-I., Nagahashi, G., and Sliwinski, B. J. (1984) *Biochem. Biophys. Res. Commun.* **122**, 1367-1373.
- Bradford, M. M. (1976) *Anal. Biochem.* **72**, 248-254.
- Hodges, T. K., and Leonard, R. T. (1974) in *Methods in Enzymology* (Fleischer, S., and Packer, L., Eds.), Vol. 32, Part B, pp. 392-406, Academic Press, New York.
- Fritz, P. J., and Hamrick, M. E. (1966) *Enzymologia* **30**, 57-64.
- Ciotti, M. M., and Kaplan, N. O. (1957) in *Methods in Enzymology* (Colowick, S. P., and Kaplan, N. O., Eds.), Vol. 3, pp. 890-899, Academic Press, New York.
- Nagahashi, G., Leonard, R. T., and Thompson, W. W. (1978) *Plant Physiol.* **61**, 993-999.
- Nagahashi, G., and Seibles, T. S. (1986) *Canad. J. Bot.* **64**, 2732-2737.
- Nagahashi, G. (1975) Isolation and Characterization of Plasma Membrane-Associated Adenosine Triphosphatase from Roots of Barley. Doctoral dissertation, University of California, Riverside.
- Giddings, J. C., Lin, H.-C., Caldwell, K. D., and Myers, M. N. (1983) *Separation Sci. Technol.* **18**, 293-306.
- Giddings, J. C. (1985) *Anal. Chem.* **57**, 945-947.